New Ferroelectrics for Naval SONAR and Modeling of Nanoscale Ferroelectric Nonvolatile Memory Materials

Alexie M. Kolpak, Ilya Grinberg, and Andrew M. Rappe
The Makineni Theoretical Laboratories, Department of Chemistry, University of Pennsylvania, Philadelphia, PA
rappe@sas.upenn.edu

Shawn T. Brown
Pittsburgh Supercomputing Center, Carnegie Mellon University, Pittsburgh, PA
stbrown@psc.edu

Abstract

Using quantum-mechanical simulations, we have computationally investigated new materials for use in Naval Sound Navigation and Ranging (SONAR). At the nanoscale, our quantum-mechanical studies show that ferroelectricity and the resultant favorable properties are stable at dimensions much smaller than previously thought. We have demonstrated that charge compensation by molecular adsorbates is more efficient than by traditional metal electrodes. This enables even a single molecular electrode to stabilize full-strength ferroelectricity in ultra-thin films and nanowires. We also report successful porting and performance tuning of our computer codes to the CRAY XT3 platform.

1. Introduction

Perovskite oxides (with formula ABO_3) have a wide range of structural, electrical and mechanical properties, making them vital materials for many technological applications, such as ultrasound machines, cell phones, and computer memory devices. Perovskite solid solutions with high piezoelectric response are of particular interest as they may be employed as sensors in SONAR devices. When such a material is deformed by underwater sound vibrations, it generates an electric field which can then be interpreted by a computer to gain information, such as depth and distance. This information is crucial for the defense and operation of Naval submarines and vessels. Other examples of perovskite oxide applications that are vital in the challenging operating conditions of the military include non-volatile ferroelectric memory for safe storage of information, and dielectric materials with tunable resonant frequency and high signal-to-noise ratio for communications devices.

Most of these materials are complex systems with some degree of disorder, making them challenging to study experimentally and theoretically. However, as it is their complexity which gives them their favorable properties, highly accurate modeling which captures the essential features of the disordered structure is necessary to explain the behavior of current materials and predict favorable compositions for new materials.

At nanoscale dimensions, ferroelectrics exhibit novel behavior, not observed in the bulk material. High-performance nanoscale ferroelectric perovskites are required for minaturization of devices and high-density nonvolatile memory storage. The processes governing the stability of polarization are not entirely understood and are now under intense experimental and theoretical investigation. Recently, a combination of methodological improvements and rise in computer speed has made first-principles calculations a viable tool for understanding these complex systems. In particular, the density functional theory (DFT) approach[1,2] offers a combination of accuracy and computational speed that may reveal the microscopic structure and interactions of complex systems.[3–5]

Rational design of new materials with improved properties requires detailed understanding of the processes that underlie the desired properties. Here, we report on our density functional simulations that develop composition-property correlations in ferroelectric perovskites. Guided by the discovered correlations between microscopic and macroscopic oxide properties, we computationally designed a new high performance piezoelectric. Accurate density functional simulations are also used to study polarization stability in ultrathin nanowires and films, demonstrating a new mechanism of charge compensation by gas-phase adsorbates. We also report our success in porting and performance tuning our codes for the Cray XT3 platform.

HPCMP Users Group Conference (HPCMP-UGC'06)
0-7695-2797-3/06 $20.00 © 2006 IEEE

2. Methodology

For all the DFT calculations presented here, we use a plane-wave basis set. Such a basis set is complete and offers the advantage of carrying out operations in both real space and reciprocal space through the use of fast Fourier transforms. Calculations are done using the standard LDA[6] exchange-correlation functional using our in-house plane wave code and the DACAPO code (http://dcwww.camp.dtu.dk/campos/Dacapo). To reduce the computational cost of the calculations we use designed non-local[7] optimized[8] and ultrasoft[9] pseudopotentials to represent the interactions of the nucleus and the core electrons with the valence electrons. Minimization of the energy with respect to the electronic degrees of freedom is done using the blocked-Davidson[10] iterative diagonalization procedure[11] with Pulay density mixing.[12] Ionic minimization is performed using a quasi-Newton algorithm.[13] DFT calculations are performed on supercells of up to 60 atoms, with a variety of atomic configurations examined to ensure accurate modeling of the disordered perovskite structures.

3. Results

3.1. Structure Property Correlations in Bi-Based Solid Solutions

Prediction of material properties from chemical composition is a fundamental goal of materials science and a vital requirement for effective computational materials design. Despite intense theoretical and experimental research[3,14–21] into technologically important ferroelectric and piezoelectric perovskite solid solutions, quantitative relationships between composition and properties are still mostly lacking. Recently, Bi perovskite alloys with $PbTiO_3$ (PT) have been shown to be promising candidates for new, lead-free or lead-reduced piezoelectrics with improved properties. In particular, high values of T_c and extremely large c/a ratios have been obtained in several $(BiBO_3)_x$-PT_{1-x} (where B = Fe, In, $Zn_{1/2}Ti_{1/2}$) solid solutions.[22–24]

Contrary to the mostly linear dependence on composition observed for Pb-based systems, ferroelectric to paraelectric transition temperatures of all $BiBO_3$-PT solid solutions exhibit strong nonlinear and often non-monotonic dependence of T_c and c/a on composition. Such surprising non-monotonic behavior is inconsistent with the intuitive expectation that an alloy's properties should be a mixture of the two end-members. The microscopic mechanisms behind these effects are currently poorly understood.[25,26] The transition temperature is of particular importance for applications, as it sets the upper temperature limit of device operation. Understanding the influence of composition on T_c is thus crucial for creating high performance devices for high operating temperature conditions.

To understand the relationships between atomic properties and overall structure, we study a series of $BiB^{2+}_{1/2}BiB^{4+}_{1/2}O_3$-PT $\left(BiB^{2+}_{1/2} = Mg, Zn;\ BiB^{4+}_{1/2} = Zr, Ti\right)$ solid solutions, which span the range of behaviors observed in $BiBO_3$-PT systems. The $Bi(Zn,Ti)O_3$-$PbTiO_3$ (BZTPT) system is of particular interest as it displays the highest T_c and c/a values of any known perovskite ferroelectric solid solution. To make sure our calculations are accurate, we compare the pair-distribution functions obtained from DFT calculations and by neutron scattering. Excellent agreement is obtained (Figure 1a).

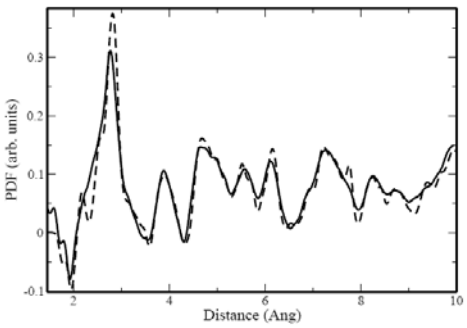

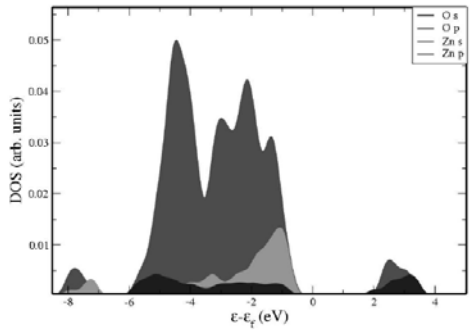

Figure 1. a) $[Bi(Zn,Ti)O_3]_x$-$[PbTiO_3)]_{1-x}$ pair distribution functions (PDF) obtained by neutron-scattering for x=0.20 (solid) and computed from relaxed DFT structures for x=0.25(dashed). The experimental and theoretical data show excellent agreement. (b) Local density of states for Zn and O in x=0.25 BZT-PT. A cutoff radius of 2 a.u. was used to perform the projection on atomic orbitals of Zn and O. Strong hybridization is present between Zn 4*p* and O 2*p* orbitals. This allows formation of short covalent Zn-O bonds and favors large Zn off-centering.

We find that a strong correlation exists between the theoretical polarizations and experimental T_c values for $BiMeO_3$-PT systems (Figure 2). This means that DFT computation of material local structure and polarization may serve as an excellent predictor of the materials properties in as of yet unexplored Bi-based perovskites.

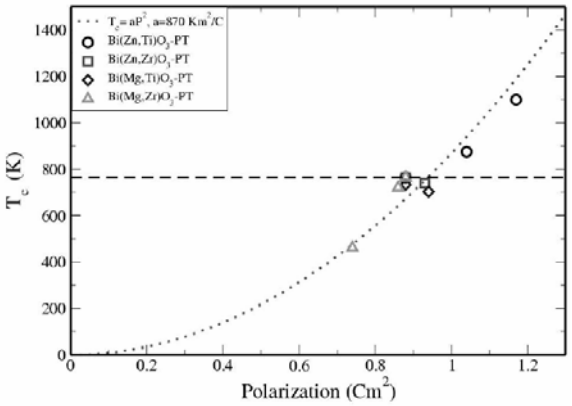

Figure 2. *P*-T_c correlation for Bi-based perovskites

To understand the chemical origin of the strong polarization, c/a and T_c enhancement in BZT-PT, we analyzed the structural and electronic properties of this material. We find that Zn off-center displacements are unusually large and favorably couple to Bi and Pb displacement, giving rise to high polarization, P, in this material. Distortions are due to the hybridization of 4*s* and 4*p* orbitals of Zn, with 2*p* orbitals of O atoms. Examination of the electronic structure through the local atom projected density of states (LDOS) method revealed that Zn 4*s* and 4*p* orbitals are partially filled in (x)BZT-(1-x)PT (Figure 1b). This is due to covalent bonding with oxygen 2*p* states and is similar to the LDOS of covalently bonded Ti ions in $PbTiO_3$ (where the hybridization is between Ti 3*d* and O 2*p*).[27] Such behavior is in stark contrast to the highly ionic bonding of Mg ions in BMT-PT which does not exhibit either high P or T_c values. Our analysis suggests that a new crystal chemical criterion of covalency should be added to complement the crystal chemical concepts of valence and ionic size.

3.2. New Piezoelectrics

Recently, we have shown that a relationship between local A-B cation interactions and phase transitions of ferroelectric perovskite solid solutions enables prediction of the compositions with optimal piezoelectric properties. In $PbTiO_3$ solid solutions, the best piezoelectric properties are exhibited at compositions at the morphotropic phase boundary (MPB), which may be predicted by

$$x_{\mathrm{PT}}^{\mathrm{MPB}} = 1 - a + b_{\mathrm{B}}^{\mathrm{avg}} - cD_{\mathrm{B}}^{\mathrm{avg}} \qquad (1)$$

where a, b, and c are constants, $R_{\mathrm{B}}^{\mathrm{avg}}$ is the average ionic size of the B-cations in the non-PT end member as computed from the B-cation composition and Shannon-Prewitt ionic radii, and D_{Ti} and $D_{\mathrm{B}}^{\mathrm{avg}}$ are distortion magnitudes for the Ti and B-cations of the non-PT end member respectively. We also showed that transition temperature at MPB is enhanced by the presence of the highly displacive Zn, Ti, and Fe ions in the non-PT end member, following

$$T_{\mathrm{c}}^{\mathrm{MPB}} = 6634 - 6539\frac{R_{\mathrm{A\text{-}O}}}{R_{\mathrm{B\text{-}O}}\sqrt{2}}, \qquad (2)$$

where $R_{\mathrm{A-O}}$ and $R_{\mathrm{B-O}}$ are the average A-and B-site cation-oxygen bond lengths.

One of the main goals of current research in piezoelectrics is the discovery of solid solutions with high T_c at the MPB. For the new systems to be technologically useful, it must be possible to synthesize a pure perovskite phase of the material under ambient conditions. The strong correlation exhibited in Figure 3 suggests that the dependence of the MPB position on the ionic size and displacements should hold for as yet unexamined Pb and Bi-based solid solutions. Below we discuss some of the solutions which should exhibit interesting properties at the MPB (Table 1). For $BiCd_{1/2}Ti_{1/2}O_3$ (BCdT), $BiZn_{1/2}Zr_{1/2}O_3$ (BZZ), $BiZn_{2/3}Nb_{1/3}O_3$ (BZN), and $BiZn_{3/4}W_{1/4}O_3$ (BZW) end-members, Eq. 2 predicts T_c^{MPB} values of ≈770 °C, 640 °C, 580 °C, and 570 °C, respectively. These compare favorably with T_c^{MPB} values of 385 °C and 440 °C for the current state-of-the-art PZT and BSPT piezoelectric, respectively. For BCdT end-member, $x_{\mathrm{PT}}^{\mathrm{MPB}}$ value is 0.52. Since the BS-PT solid solution is stable in the perovskite phase up to 0.5 BS content, the prospects for synthesizing MPB compositions with very high Curie temperatures in this system are more promising.

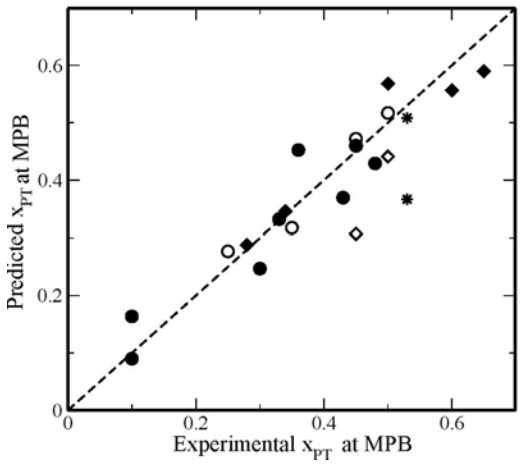

Figure 3. Correlation between the mole fractions of PT at MPB predicted by Eq. 1 and mole fractions of PT at MPB observed experimentally. Solid solutions for which we have DFT B-cation displacement data are marked by filled circles and diamonds for Pb-based and Bi-based systems respectively. MPB positions predicted for Pb-and Bi-based systems where B-cation displacement data is estimated are marked by open circles and diamonds respectively.

Table 1. Predicted x_{PT}^{MPB} and T_c^{MPB} values for BiB' $B''$$O_3$-PT solid solutions. Predicted x_{PT}^{MPB} are obtained using Eq. 1. T_c^{MPB} (in °C) are obtained by using Eq. 2. Ionic size and displacement data in Å.

g	B', B'' size	B', B'' disp.	t	x_{PT}^{MPB} predict	T_c^{MPB} predict
$BiInO_3$	0.80,0.80	0.07,0.07	0.887	0.67	507
$BiCd_{1/2}Ti_{1/2}O_3$	0.95,0.60	0.08,0.25	0.897	0.54	770
$BiZn_{2/3}Nb_{1/3}O_3$	0.74,0.64	0.25,0.17	0.926	0.26	579
$BiZn_{3/4}W_{1/4}O_3$	0.74,0.60	0.25,0.10	0.927	0.30	572

3.3. Ferroelectricity in Ultra-Thin $PbTiO_3$ Films

Ferroelectric materials have ideal properties for use in non-volatile memory devices: Due to atomic displacements in the minimum energy crystal structure, ferroelectric materials have a spontaneous electric polarization which remains stable in the absence of an external electric field. The direction of this polarization may be switched by applying an electric field, that results in two distinct, stable states, that may easily be translated into the binary 1's and 0's used in data storage.

The properties of ferroelectric materials are currently being utilized in some non-volatile memory storage applications, for example, non-volatile random access memories (NVRAM), where electrode/ferroelectric/ electrode layers are incorporated into traditional CMOS devices. Compared to other existing non-volatile technologies such as Flash and EEPROM's (electrically erasable and programmable read-only memories), ferroelectric NVRAM (FERAM) requires low power consumption and short-programming times, making it very attractive. Available FERAM technology has a significant disadvantage, however, in that the currently attainable transistor density in FERAMs is quite low. To fully realize the potential of FERAM, it is therefore of great importance to design and fabricate increasingly higher-density devices composed of nanoscale ferroelectric components. Such efforts require a much greater understanding of the behavior of ferroelectric nanomaterials, which can differ significantly from their bulk counterparts.

Some of the most pressing questions associated with the behavior of ferroelectric nanomaterials concern their ability to retain a stable polarized ground state at the smallest dimensions. In a ferroelectric perovskite, the cations displace from the centers of their octahedral oxygen cages, producing a small electric dipole per unit cell. Dipoles in neighboring unit cells tend to align in the same direction to minimize energy, collectively giving rise to a significant macroscopic polarization. In a film, the resulting electrostatics may be modeled by considering the two film surfaces as sheets of charge of opposite sign. These charge sheets set up an electric field opposing the polarization. In the limit of an infinitely thick film, the magnitude of this field is negligible, but as the film thickness approaches the nanoscale, the field known as the depolarizing field, becomes quite large.

In a ferroelectric capacitor geometry, such as that used in FERAMs, most of the surface charge is in fact screened by the metal electrodes sandwiching the film. However, even this small amount of uncompensated charge (due to the inherent screening length of the metal) may produce a depolarizing field strong enough to suppress or eliminate the polarization in nanosize ferroelectrics,[28–31] significantly decreasing T_c, and removing their utility as nonvolatile memory elements. Therefore, it is vital to the future development of high-density FERAM and other technologies to determine the size-dependent behavior of ferroelectric materials, and to understand how charge is screened at ferroelectric interfaces.

We have recently gained insights in this area by studying the size-dependent stability of ultrathin ferroelectric $PbTiO_3$ films supported on $SrRuO_3$ electrodes, that were experimentally observed to retain polarization at much smaller dimensions than expected from previous theoretical and experimental data.[32] We proposed a new screening mechanism in which atomic and molecular adsorbates compensate the surface polarization charge. Using DFT to model a series of films between 8 and 20 Å (2 to 5 unit cells) in thickness, we found that an overlayer of adsorbates stabilizes bulk-like polarization at all thicknesses, with the identity of the adsorbate determining the polarization direction. Electronegative adsorbates (O and OH) enforce a positive polarization (towards the adsorbates) while electropositive adsorbates (H, CO_2) induce a negative polarization. For example, a representative structure of a three-unit-cell-thick film with OH adsorbates is shown in Figure 4. The figure illustrates a clear ferroelectric displacement pattern throughout the film, with a bulk-like polarization.

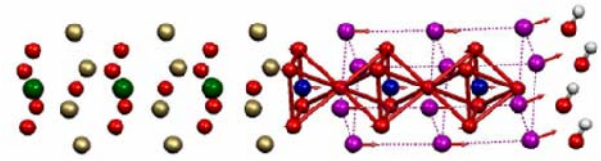

Figure 4. Relaxed structure of a three-unit-cell-thick $PbTiO_3$ film. The polarization charge is compensated by a metallic $SrRuO_3$ electrode at the negative surface (left), while an over-layer of OH adsorbates screens the positive surface (right). Pb, Ti, O, Sr, Ru, and H atoms are shown in purple, blue, red, gold, green, and white, respectively. The black arrows indicate the ferroelectric displacements of each atom.

To determine the thermodynamic stability of the films under experimental temperatures and pressures, we compute the Gibbs free energy, $\Delta G = \Delta H - T\Delta S = \Delta E + p\Delta V - T\Delta S$, of each adsorption reaction. The change in enthalpy, ΔH, is estimated by adding $p\Delta V \approx -k_B T$ to the DFT-computed chemisorption energy, ΔE, with corrections for zero-point energy and spin-polarization included for OH adsorbates. The entropy contribution to the adsorption reaction, $T\Delta S$, is primarily due to the difference in the vibrational entropy of the adsorbates, computed directly from the DFT values of the vibrational modes, and the entropy of the adsorbate in the gas phase (obtained from experimental data tabulated at http://webbook.nist.gov/chemistry). Computing ΔG as a function of temperature at the experimental H_2O and O_2 gas pressures ($p_{H_2O} = 5 \times 10^{-7}$ bar, $p_{O_2} = 3.3 \times 10^{-3}$ bar) determines OH to be the most stable adsorbate. Furthermore, the temperature at which OH adsorption becomes thermodynamically unfavorable, $T_{crossover}$, is shown to be in the range of the experimental T_C for a given film thickness. The values of $T_{crossover}$ and ΔE are given in Table 2 for films of various thicknesses.

Table 2. ΔE and $T_{crossover}$ for OH adsorption on $SrRuO_3$-supported $PbTiO_3$ films of n = 2 to 5 unit cells thick. For comparison, the experimentally determined values of T_C were found to be ≈ 700 and 825 K for n = 3 and 5, respectively.

n	ΔE	$T_{crossover}$
2	-2.09	500
3	-2.19	580
4	-2.42	740
5	-2.64	900

Our results demonstrate that adsorbates may be successfully used as a second electrode, inducing strong polarization and retaining thermodynamic stability at experimentally and technologically accessible temperatures and pressures.

3.4. Single Electrode Stabilization of Ferroelectricity in $BaTiO_3$ Nanowires

We have extended the above work in another recent publication,[33] in which we investigated the experimentally observed $1/d_{nw}$ (where d_{nw} is the nanowire diameter) scaling of the transition temperature in $BaTiO_3$ nanowires. In this study, nanowires with diameters as thin as ≈ 30 nm were shown to exhibit stable ferroelectric polarization at and above room temperature, as illustrated in Figure 5, and even wires with diameters as thin as two unit cells were predicted to remain ferroelectric at lower temperatures.

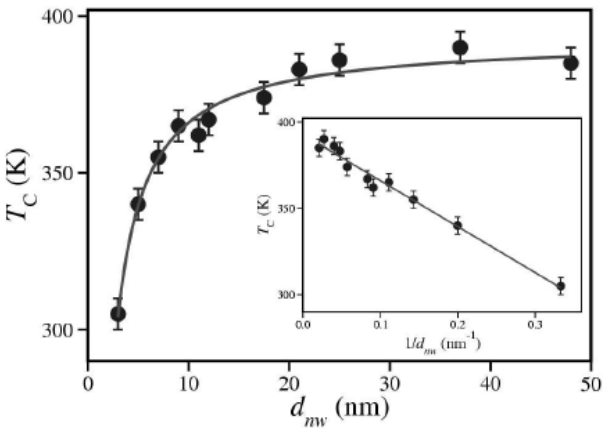

Figure 5. Experimental dependence of T_C on the nanowire diameter, d. While the thinnest wire shown here, with $d \approx 3$ nm, has a value of T_C above room temperature, estimating T_C for a comparable $SrRuO_3/BaTiO_3/SrRuO_3$ film from theoretical computations in Reference 26 gives value $T_C \approx 7$ K.

Using DFT and thermodynamic modeling, we found that, similarly to the $SrRuO_3/PbTiO_3$/OH films discussed above, $BaTiO_3$ films supported on a single Au electrode were stabilized by O, H, and OH overlayers, with OH molecules as the thermodynamically favored adsorbate. (Both films and nanowires were shown to behave similarly as one-dimensional systems characterized by the thickness or diameter. To decrease computational expense, films were used in most of the study.) Furthermore, our work showed that a layer of molecular adsorbates on one surface was sufficient to stabilize strong polarization in the absence of a second electrode. Figure 5 shows a representative 4-unit-cell-thick $BaTiO_3$ film with OH adsorbates, that illustrates the bulk-like ferroelectric displacement pattern in the central region, and polarization enhancement at the $BaTiO_3$/OH interface. The bottom, vacuum/$BaTiO_3$ interface is compensated only via intrinsic screening.

The results demonstrate that a single electrode composed of molecular adsorbates is much more efficient at screening the polarization charge in $BaTiO_3$ than metallic electrodes. For instance, the thinnest $SrRuO_3/BaTiO_3/SrRuO_3$ film to exhibit a non-zero polarization at T = 0 K was recently shown to be 8 unit cells thick, with the polarization only a small fraction of the bulk value. Our work therefore suggests the possibility of effective new design principles for the fabrication of high-density non-volatile memory devices.

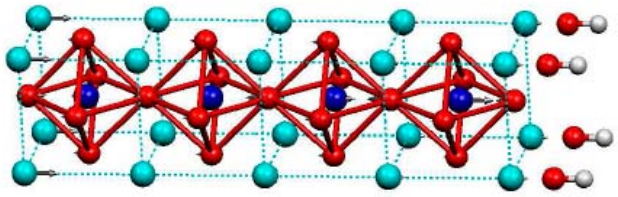

Figure 6. Relaxed structure of a four-unit-cell-thick $BaTiO_3$ film with an overlayer of OH adsorbates on the positive surface. Even without a bottom electrode, the film is found to have a bulk-like ferroelectric displacements in the central layers.

3.5. Cray XT3 Port

During the course of the past year, we have ported our plane-wave code to the XT3 platform. Our program contains approximately 9,500 lines of code and makes calls to several mathematical libraries, making the porting and optimizing performance a non-trivial task. The results for several benchmarks were tested and compared against typical production platforms such as Pentium 4 Xeon Beowulf Cluster and the SGI O3K computers. Agreement to six decimal places between the XT3 and other platforms was achieved. We are currently using the XT3 in production mode and working on optimizing scratch disk and memory usage to get further speed-up.

4. Conclusion

Using first-principles DFT calculations, we have investigated the properties of ferroelectric materials. For bulk piezoelectrics, relationships between atomic composition, electronic structure, and technologically important properties were elucidated. These offer guidance for the design of new piezoelectric materials with superior performance. In our studies of thin-film ferroelectrics, we have demonstrated a new mechanism of charge passivation at the ferroelectric surface by molecular and atomic adsorbates. This effect reduces the critical thickness at which ferroelectricity is stable to 1 nanometer, enabling further miniaturization of nonvolatile ferroelectric memory devices. To take advantage of the newest computational resources of the HPCMP program, we have ported and optimized our density functional codes for the Cray XT3 system.

5. Significance to DoD

The perovskite oxides are used extensively in modern Naval SONAR devices, non-volatile memories and telecommunications applications. The US Navy would reap a considerable military advantage from developing SONAR-detecting materials and microwave materials with higher performance, lower cost, and less harmful environmental side effects. Understanding the behavior of current perovskite oxides is critical for the goal of developing new materials. Once the relationship between the atomic composition, structure and material properties are understood, new materials that improve upon existing technology may be designed. Our DFT calculations have revealed the microscopic origin of transition temperature that sets the operating range of piezoelectric devices and suggested a series of new promising compositions for next-generation piezoelectric materials. Our demonstration of adsorbate stabilization of ferroelectricity in ultrathin ferroelectrics suggests that atomic and molecular adsorbates are more effective than metallic electrodes in stabilizing the ferroelectric stability of nanoscale domains; suggesting new design principles for ferroelectric memory devices and new applications for ferroelectrics as gas sensors.

Acknowledgements

The authors would like to thank P.K. Davies for many useful discussions. We would also like to thank Larry P. Davis, Phil Bucci and ARSC, and ERDC for supporting the Cray X1 porting and performance tuning project.

This work was supported by the Office of Naval Research under grant number N-000014-00-1-0372 and through the Center for Piezoelectrics by Design. We also acknowledge the support of the National Science Foundation, through the MRSEC program, grant No. DMR 0409848. Computational support was provided by the High-Performance Computing Modernization Program of the Department of Defense and the Center for Piezoelectrics by Design. Correspondence and requests for materials should be addressed to A.M.R. (email: rappe@sas.upenn.edu)

Systems Used

ERDC SGI3900, Cray XT3 and Cray X1, ARSC X1, AHPCRC Cray X1

CTA

Computational Materials Science (CMS)

References

1. Hohenberg, P. and W. Kohn, *Phys. Rev.*, 136, B864, 1964.

2. Kohn, W. and L.J. Sham, *Phys. Rev.*, 140, A1133, 1965.

3. Grinberg, I., V.R. Cooper, and A.M. Rappe, *Nature*, 419, 909, 2002.

4. Fu, H. and R.E. Cohen, *Nature*, 402, 281, 2000.

5. George, A.M., J. Iniguez, and L. Bellaiche, *Nature*, 413, 54, 2001.

6. Perdew, J.P. and A. Zunger, *Phys. Rev. B*, 23, 5048, 1981.

7. Ramer, N.J. and A.M. Rappe, *Phys. Rev. B*, 59, 12471, 1999.

8. Rappe, A.M., K.M. Rabe, E. Kaxiras, and J.D. Joannopoulos, *Phys. Rev. B Rapid Comm.*, 41, 1227, 1990.

9. Vanderbilt, D., *Phys. Rev. B Rapid Comm.*, 41, 7892, 1990.

10. Davidson, E.R, *J. Comput. Phys.*, 17, 87, 1975.

11. Bendtsen, C., O.H. Nielsen, and L.B. Hansen, *Appl. Num. Math.*, 37, 189, 2001.

12. Pulay, P., *J. Comp. Chem.*, 3, 556, 1982.

13. Pfrommer, B.G., M. Cot´e, S.G. Louie, and M.L. Cohen, *J. Comp. Phys.*, 131, 233, 1997.

14. Eitel, R.E., C.A. Randall, T.R. Shrout, P.W. Rehrig, W. Hackenberger, and S.-E. Park, *Jpn. J. Appl. Phys.*, 40, 5999, 2001, ISSN 0021-4922, URL http://dx.doi.org/10.1143/JJAP.40.5999.

15. Cheng. J.R., R.E. Eitel, and L.E. Cross, *J. Am. Ceram. Soc.*, 86, 2111, 2003.

16. Bellaiche, L., A. Garcia, and D. Vanderbilt, *Phys. Rev. Lett.*, 84, 5427, 2000.

17. Niguez, J.I., D. Vanderbilt, and L. Bellaiche, *Phys. Rev. B*, 67, 224107, 2003.

18. Halilov, S.V., M. Fornari, and D.J. Singh, *Appl. Phys. Lett.*, 81, 3443, 2002.

19. Halilov, S.V., M. Fornari, and D.J. Singh, *Phys. Rev. B*, 69, 174107, 2004.

20. Suchomel, M.R. and P.K. Davies, *J. Appl. Phys.*, 96, 4405, 2004.

21. Juhas, P. and P.K. Davies, *J. Am. Ceram.*, Soc., 87, 2086, 2004.

22. Randall, C.A., R. Eitel, B. Jones, T.R. Shrout, D.I. Woodward, and I.M. Reaney, *J. Appl. Phys.*, 95, 3633, 2004.

23. Suchomel, M.R. and P.K. Davies, *Appl. Phys. Lett.*, 86, 262905, 2005.

24. Duan, R., R.F. Speyer, E. Alberta, and T.R. Shrout, *J. Mater. Res.*, 19, 2185, 2004.

25. Isupov, V.A., *Physica Status Solidi A -Appl. Res.*, 181, 211, 2000.

26. Stephanovich, V.A., M.D. Glinchuk, and C.A. Randall, *Phys. Rev. B*, 70, 134101, 2004.

27. Cohen, R.E., *Nature*, 358, 136, 1992.

28. Junquera, J. and P. Ghosez, *Nature*, 422, 506, 2003.

29. Sai, N., A.M. Kolpak, and A.M. Rappe, *Phys. Rev. B Rapid Comm.*, 72, 020101(R, 2005.

30. Meyer, B. and D. Vanderbilt, *Phys. Rev. B*, 63, 205426 1, 2001.

31. Mehta, R.R., B.D. Silverman, and J.T. Jacobs, J. *Appl. Phys.*, 44, 3379, 1973.

32. Fong, D.D., A.M. Kolpak, J.A. Eastman, S.K. Streiffer, P.H. Fuoss, G.B. Stephenson, C. Thompson, D.M. Kim, K.J. Choi, C.B. Eom, et al., *Phys. Rev. Lett.*, 96, 127601, 2006.

33. Spanier, J.E., A.M. Kolpak, J.J. Urban, W.S. Yun, L. Ouyang, I. Grinberg, A.M. Rappe, and H. Park, *Nano Lett.*, 6, 735, 2006.